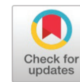

Atomic layer deposition of BN as a novel capping barrier for B_2O_3

Aparna Pilli,[1] Jessica Jones,[1] Natasha Chugh,[1] Jeffry Kelber,[1,a)] Frank Pasquale,[2] and Adrien LaVoie[2]
[1]*Department of Chemistry, University of North Texas, Denton, Texas 76203*
[2]*Lam Research Corporation, Tualatin, Oregon 97062*

(Received 14 February 2019; accepted 14 May 2019; published 5 June 2019)

The deposition of boron oxide (B_2O_3) films on Si and SiO_2 substrates by atomic layer deposition (ALD) is of growing interest in microelectronics for shallow doping of high aspect ratio transistor structures. B_2O_3, however, forms volatile boric acid (H_3BO_3) upon ambient exposure, requiring a passivation barrier, for which BN was investigated as a possible candidate. Here, the authors demonstrate *in situ* deposition of BN by sequential BCl_3/NH_3 reactions at 600 K on two different oxidized boron substrates: (a) B_2O_3 deposited using BCl_3/H_2O ALD on Si at 300 K ("B_2O_3/Si") and (b) a boron-silicon oxide formed by sequential BCl_3/O_2 reactions at 650 K on SiO_2 followed by annealing to 1000 K ("B-Si-oxide"). X-ray photoelectron spectroscopy (XPS) data demonstrate layer-by-layer growth of BN on B_2O_3/Si with an average growth rate of ∼1.4 Å/cycle, accompanied by some B_2O_3 removal during the first BN cycle. In contrast, continuous BN growth was observed on B-Si-oxide without any reaction with the substrate. XPS data also indicate that the oxide/nitride heterostructures are stable upon annealing in ultrahigh vacuum to >1000 K. XPS data, after the exposure of these heterostructures to ambient, indicate a small amount of BN oxidation at the surface NH_x species, with no observable hydroxylation of the underlying oxide films. These results demonstrate that BN films, as thin as 13 Å, are potential candidates for passivating boron oxide films prepared for shallow doping applications. *Published by the AVS.*
https://doi.org/10.1116/1.5092806

I. INTRODUCTION

Boron oxide (B_2O_3) films have been proposed for ultrashallow Si doping applications in advanced CMOS fabrication.[1–4] Layer-by-layer growth of B_2O_3 by atomic layer deposition (ALD) allows for precise thickness control of the conformal B_2O_3 layers, which, in turn, is proportional to the B dopant concentration in the Si substrates.[1,2] We have previously demonstrated the ALD of B_2O_3 films on Si by alternating exposures of BCl_3 and H_2O precursors at room temperature.[5] Additionally, sequential reactions of BCl_3 and O_2 on SiO_2 at 650 K yielded a mixed B-oxide/Si-oxide, which, upon annealing at 1000 K in ultrahigh vacuum (UHV), removed Cl, leaving B-Si-oxide.[5]

The use of boron oxide for doping applications motivates the use of a capping/diffusion barrier to protect the oxide against reaction upon exposure to ambient and the formation of boric acid.[1–3,6] Previous reports of capping barriers include antimony oxide,[2,4] alumina,[1,6] and silicon dioxide.[3] Antimony oxide does not passivate B_2O_3 in ambient conditions; after long term storage, the thickness of both the underlying boron oxide and antimony oxide layers increased, which the authors attribute to diffusion of water vapor through the capping barrier.[2,4] Kalkofen *et al.* reported ∼44% reduction in B_2O_3 thickness after depositing the antimony oxide cap at 473 K.[2] This loss in the thickness of B_2O_3 was attributed to the elevated temperature used for cap deposition.[2] Alumina has been reported to crack when used as a capping barrier at temperatures >673 K, allowing the B_2O_3 under-layer to oxidize to boric acid.[6] Boron was reported to selectively diffuse into the silicon dioxide sidewall spacer instead of Si during rapid thermal anneal (RTA) treatment at 1273 K.[7] RTA is generally used for activating existing dopants or doping substrates. Silicon dioxide as a capping barrier may result in a significant loss of B dose from Si. Capping B_2O_3 with BN provides a novel route to the passivation of the oxide surface. Although the thermal stability of BN prevents its use for doping by drive-in anneal into the Si substrate,[1] BN acts as an excellent passivation barrier for B_2O_3 and may also inhibit upward boron migration during drive-in anneal.

Previously, BN was deposited by thermal, plasma, and laser ALD methods using various precursors.[8–17] The first study of BN ALD reported the use of BBr_3 and NH_3 precursors at substrate temperatures ranging from 673 to 1023 K.[9] This was followed by other reports using the same precursors for laser ALD of BN on SiO_2,[10] and a more recent report of thermal ALD on nanoporous aluminum oxide templates.[11] Ferguson *et al.* described the growth of BN using BCl_3/NH_3 ALD at 500 K on ZrO_2 substrates.[12] Thermal and plasma ALD of BN using noncorrosive precursors was also established when triethylborane[13] and triethylborate[14] were used in conjunction with NH_3 (Ref. 13) and N_2/H_2 plasma,[14] respectively.

ALD of BN using BCl_3 and NH_3 precursors at elevated temperatures (600 K) is a well-explored procedure.[12,15–17] We present *in situ* x-ray photoelectron spectroscopy (XPS) data demonstrating that sequential BCl_3/NH_3 exposures at 600 K yield BN film growth on (a) B_2O_3/Si and (b) B-Si-oxide, with some erosion of the substrate oxide in the former case but not the latter. Here, the notation "B_2O_3/Si" denotes B_2O_3 films deposited by BCl_3/H_2O precursors on a

[a)]Electronic mail: Kelber@unt.edu

Si substrate at 300 K; and "B-Si-oxide" describes boron-silicon oxide films formed by sequential BCl_3/O_2 reactions at 650 K on SiO_2 followed by annealing to 1000 K. Additionally, XPS data before and after BN/oxide exposure to ambient demonstrate the ability of BN films, that are a few monolayers thick, to passivate such oxides against ambient exposure. These nitride/oxide interfaces are also thermally stable to at least 1000 K in UHV. These results demonstrate that ultrathin BN films can be grown on boron oxide substrates by ALD and show significant promise as capping/diffusion barriers for B_2O_3 in shallow doping applications.

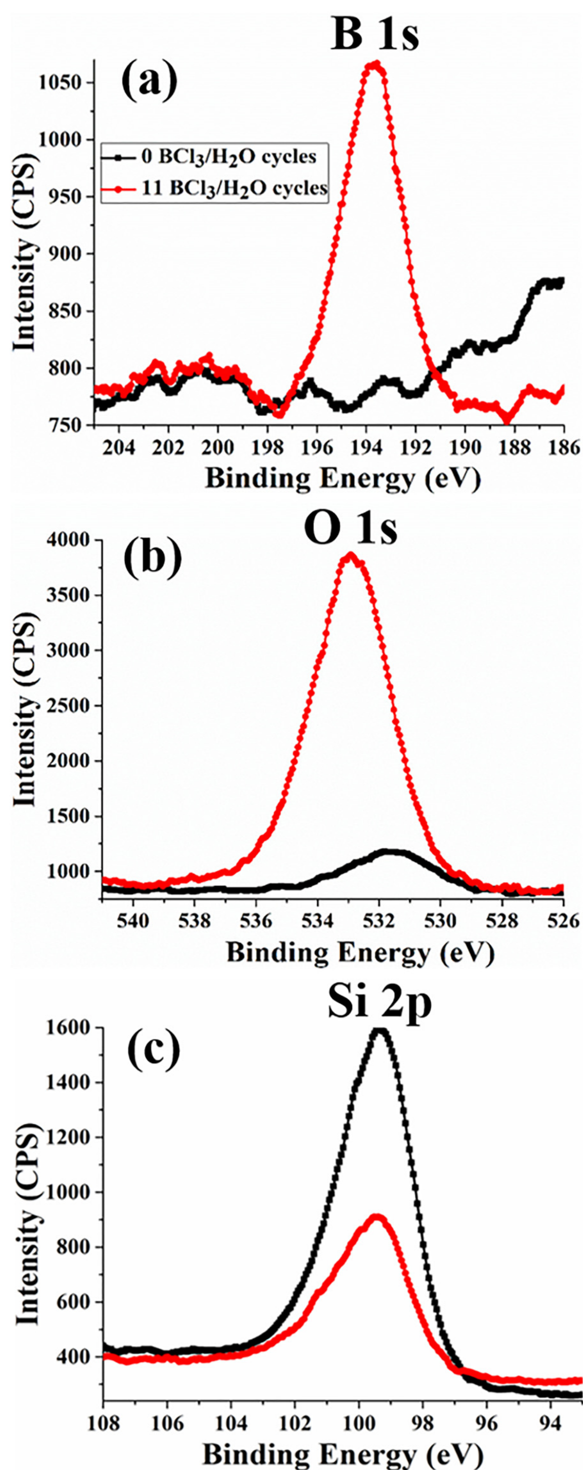

FIG. 1. XPS spectra of (a) B 1s and Cl 2p regions, (b) O 1s regions, and (c) Si 2p regions of Si(100) before exposure to BCl_3/H_2O (black square trace) and after 11 cycles of BCl_3/H_2O at 300 K, resulting in a B_2O_3 film on Si (red circle trace).

II. EXPERIMENT

Si substrates ($1 \times 1\ cm^2$) were scribed from an undoped Si(100) wafer. *Ex situ* cleaning was performed by sonication in methanol (Fisher Scientific, >99.99% purity, CAS# 67-56-1) and then in acetone (Fisher Scientific, HPLC grade, CAS# 67-64-1) for 10 and 5 min, respectively, prior to piranha cleaning (5:1:1, H_2O:H_2SO_4:H_2O_2) to remove organic contaminants. This was followed by an HF dip (300:1, H_2O:HF) to remove most of the native oxide on silicon. The HF etch step was done on one of the samples—sample (a) used for B_2O_3 ALD denoted as B_2O_3/Si. This step was skipped for sample (b) denoted as B-Si-oxide.

After *ex situ* cleaning, the sample was transferred to a stainless steel three chamber vacuum system which has been described previously.[5] Briefly, the system is equipped with an ALD chamber (base pressure $\sim 1 \times 10^{-7}$ Torr), an MBE deposition chamber (base pressure $\sim 5 \times 10^{-10}$ Torr), and a surface analysis chamber (base pressure $\sim 3 \times 10^{-10}$ Torr) with capabilities for XPS and an Ar^+ ion sputter gun for sample cleaning. These chambers were isolated by manually operated gate valves, and sample transfer between chambers was accomplished using a magnetically coupled transfer arm without sample exposure to ambient. Sample heating in the ALD or surface analysis chamber was accomplished using resistive heaters, and temperature measurements were made by a type K thermocouple mounted in proximity to the sample. Gas pressure in the sample analysis chamber was monitored using a nude ion gauge calibrated for N_2. Pressure in the ALD chamber was monitored using either a nude ion gauge or a baratron capacitance manometer. ALD exposures recorded here are in Langmuir (L; $1\ L = 10^{-6}$ Torr sec) and have not been corrected for ion gauge sensitivity or flux to the surface.

For sample (a), *in situ* substrate cleaning was carried out by annealing in O_2 (10^{-7} Torr, 1000 K) (AirGas, 99.999% purity, CAS# 7752-44-7) to remove adventitious C. Si substrates were subsequently exposed to 5×10^{-5} Torr Ar^+ (Scott Specialty Gases, 99.9999% purity, CAS# 7440-37-1) ions at 3 kV, 25 mA sputter conditions to remove the surface oxygen. Si samples used here typically had O surface coverages of ~2 Å, and XPS data indicated the presence of Si^0 and a small amount of suboxide, but no Si^{4+}.[18,19] The *in situ* cleaning process for sample (b) was achieved by annealing in UHV at 1000 K for 1 h to remove surface carbon contamination. The cleaned SiO_2 substrate had carbon impurity levels of ≤1 at. %.

XPS spectra were acquired using a 100 mm mean radius hemispherical analyzer set at a constant pass energy of 50 eV, a nonmonochromatic Al Kα x-ray source (1486.6 eV) operating at 300 W and 15 kV, and with a sampling area of $\sim 5\ mm^2$. All photoemission binding energies were referenced to the

bulk Si 2p feature at 99.3 eV.[18,19] The spectra were analyzed using commercially available software with capabilities for Shirley background subtraction, and the peaks were fit using Gaussian–Lorentzian functions.[20] Film thicknesses were averaged over the x-ray spot size and calculated using inelastic mean free path (IMFP) lengths through the BN overlayer; 34.4, 27.16, 30.06, and 34.29 Å for B 1s, O 1s, N 1s, and Cl 2p photoelectrons, respectively. B_2O_3 thickness after BN deposition was calculated using the IMFP lengths through the B_2O_3 overlayer; 34.93, 26.03, and 33.04 Å for Si 2p, O 1s, and B 1s, respectively. The IMFP lengths were calculated using TPP-2M IMFP predictive equation.[21]

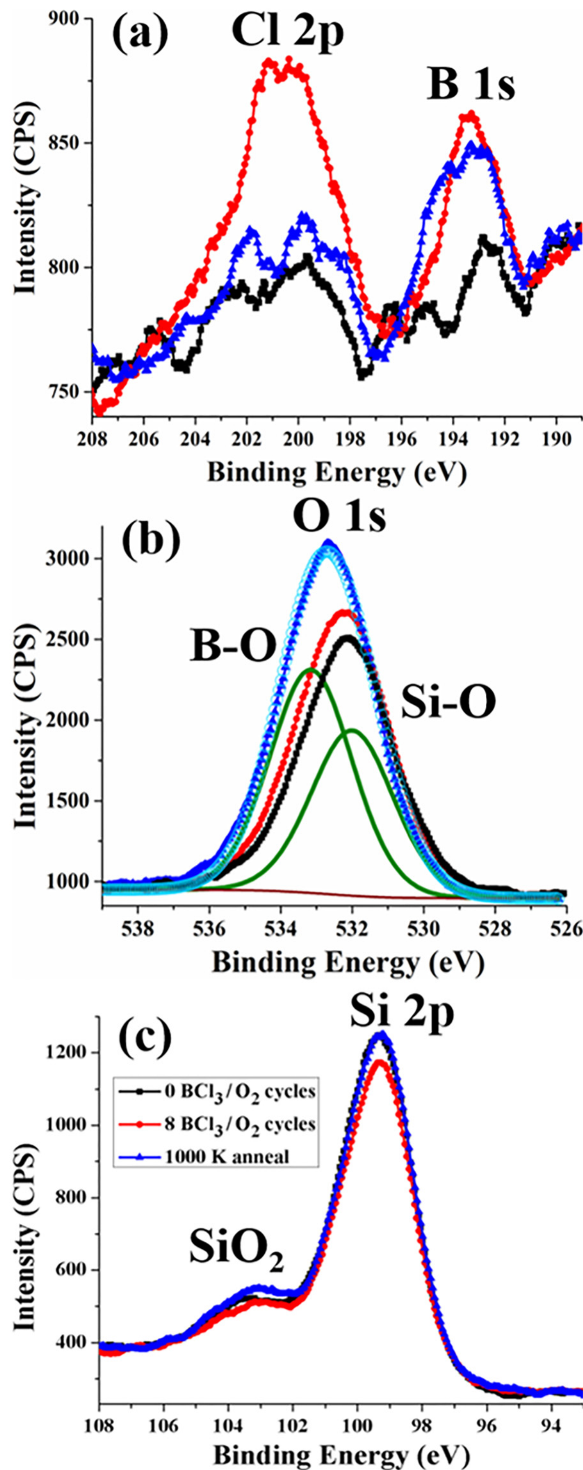

FIG. 2. XPS spectra of (a) B 1s and Cl 2p, (b) O 1s regions, and (c) Si 2p regions of B-Si-oxide films after 0 BCl_3/O_2 reactions (black square trace), 8 BCl_3/O_2 reactions at 650 K on SiO_2 (red circle trace), and after 1 h UHV anneal to 1000 K (blue triangle trace). In (b), the deconvoluted O 1s spectrum after annealing indicates the presence of both B–O (solid green trace) and Si–O (solid green trace) features at 533.5 and 532.3 eV, respectively. The sum of the deconvoluted spectra (light blue open circles) is in close agreement with experimental data (blue triangle trace).

Electronic grade BCl_3 (IGX Group, CAS# 10294-34-5, 99.999% purity) and NH_3 (Praxair, CAS# 7664-41-7, >99.999% purity) gases obtained from commercial vendors were used as precursors without further purification. BN films were deposited *in situ* on B_2O_3 by alternating BCl_3 (7.5×10^7 L) and NH_3 (4.2×10^7 L) exposures at 600 K. The boron oxide films examined here were grown on two different substrates—Si and SiO_2—as described previously.[5] Our previous study indicated that B_2O_3 growth using BCl_3/H_2O cycles occurred at 300 K on Si by an ALD process, but the growth on SiO_2 using BCl_3/O_2 did not occur at 300 K but did occur at 650 K in large part by B reaction with the oxide substrate.[5] That study also showed that B_2O_3 growth on Si occurred with Cl contamination only at the boron oxide/Si interface but the growth on SiO_2 yielded significant Cl contamination throughout the boron oxide film, which could be removed by annealing.[5] Attempted BN growth on each type of boron oxide permits an examination of whether factors such as Cl contamination or the proximity of the substrate might influence BN growth or the ability of BN to passivate the substrate. During both BN and B_2O_3 growth, the chamber was allowed to pump down to a base pressure of 3×10^{-5} Torr between alternate cycles. All postdeposition anneals were performed in the UHV chamber with a base pressure of $\sim 3 \times 10^{-10}$ Torr.

III. RESULTS

A. B_2O_3 deposition on Si and SiO_2

Thin films of boron oxide were deposited on Si and SiO_2 substrates by alternating exposures of BCl_3/H_2O at 300 K and BCl_3/O_2 at 650 K, respectively. A detailed description of the respective B_2O_3 and B-Si-oxide growth processes has been reported previously.[5] The XPS spectra of B 1s, O 1s, and Si 2p regions corresponding to B_2O_3 ALD on Si after 11 BCl_3/H_2O exposures at 300 K are displayed in Figs. 1(a)–1(c). These data indicate that the average thickness of B_2O_3 is $\sim 25.6 \pm 1.4$ Å after 11 ALD cycles with a B 1s binding energy at ~193.8 eV. This is consistent with the previously reported values for B–O bond formation, although this information cannot be used to rule out the formation of boric acid (H_3BO_3).[22] Previous studies[5,23] have reported the presence of a small Cl 2p feature near 201.4 eV due to Cl–Si bond formation at the B_2O_3/Si interface, as Cl–Si species are unreactive toward H_2O at room temperature.[5] The data in Fig. 1(a), however, indicate a negligible change in intensity in this region after B_2O_3 ALD, suggesting that the presence of any adsorbed Cl is small and masked by the plasmon feature of the substrate.[24]

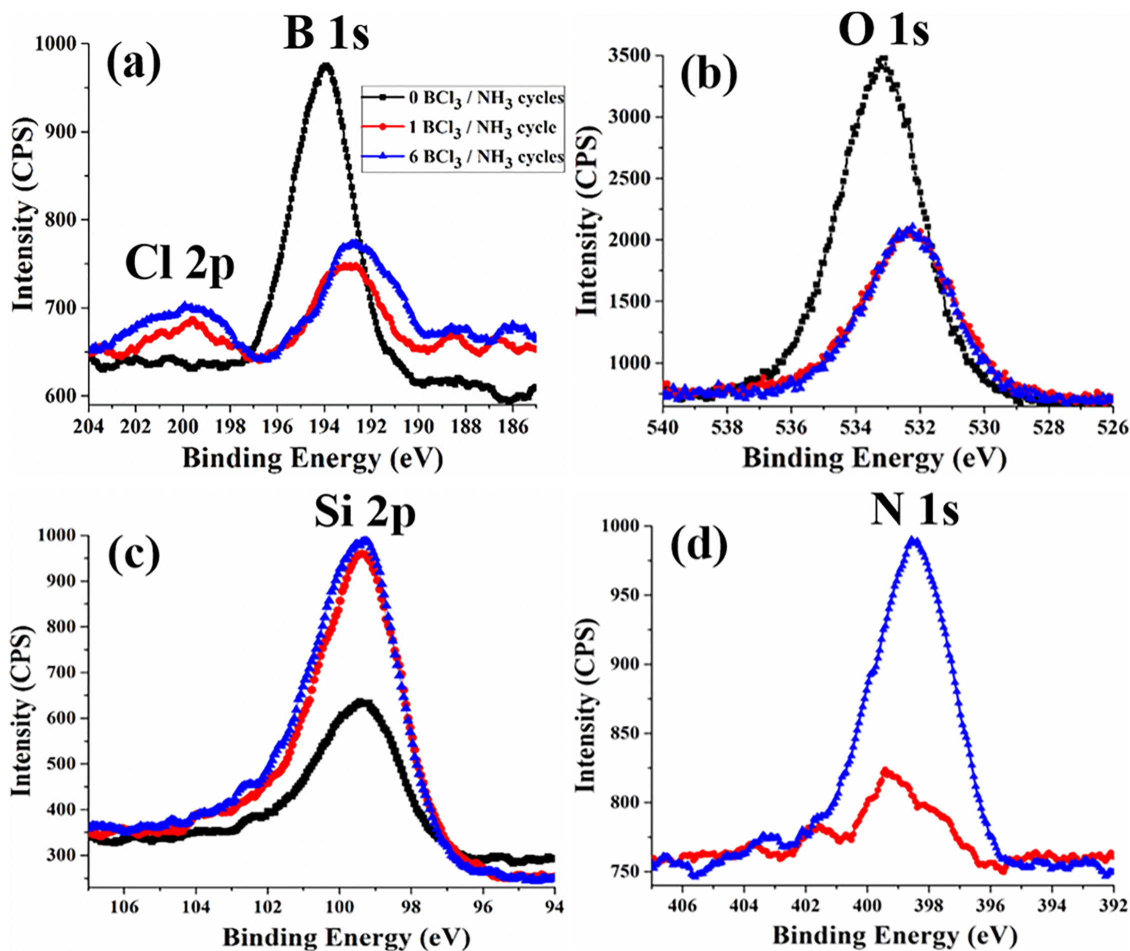

FIG. 3. Evolution of (a) B 1s and Cl 2p, (b) O 1s, (c) Si 2p, and (d) N 1s XPS spectra during BN ALD on a 25.6 Å thick B_2O_3/Si film. After 0 BCl_3/NH_3 cycles (black square trace), after 1 BCl_3/NH_3 cycle (red circle trace), and after 6 BCl_3/NH_3 cycles (blue triangle trace) at 600 K.

The XPS spectra of B 1s, O 1s, and Si 2p regions corresponding to boron oxide deposited on SiO_2 after 8 BCl_3/O_2 cycles at 650 K, followed by annealing to 1000 K in UHV, are displayed in Figs. 2(a)–2(c), respectively. Figure 2(a) shows an increase in the B 1s intensity at ~193.3 eV corresponding to B–O bonds after 8 BCl_3/O_2 cycles. This was accompanied by an increase in the Cl contamination at ~200.8 eV, indicating that the O_2 precursor failed to completely abstract Cl from the boron oxide film even at an elevated substrate temperature. An initial UHV anneal of the films to ~800 K removed some Cl contamination but a significant amount of Cl was still incorporated in the film. A subsequent anneal to 1000 K significantly decreased the Cl contamination as seen in Fig. 2(a). This anneal temperature agrees well with the desorption temperature used for halogen removal from Si under UHV conditions.[25] The anneal treatment also resulted in a slight broadening of the B 1s signal toward higher binding energy. The full width at half maximum (FWHM) of the B 1s peak increased from 2.1 to 2.7 eV [Fig. 2(a)]. This is consistent with the removal of surface contamination and the formation of a mixed boron-silicon oxide, which is stable at 1000 K. The XPS-derived thickness of the oxidized B phase after anneal is ~7.8 ± 0.2 Å.

Figure 2(b) shows an increase in the O 1s intensity and a shift to higher binding energy from ~532 to ~532.7 eV after the UHV anneal. The increase in O 1s intensity after the anneal step could be due to the reappearance of O 1s signal, which has been attenuated by Cl contamination. The significant change in intensity, however, points to the replacement of Cl atoms with adsorbed O or O migration from the underlying substrate. The shift in O 1s spectra to higher binding energies also agrees well with Si–O–B formation.[26]

The broad O 1s XPS spectrum, after the anneal, is deconvoluted into two peaks using FWHM and binding energy constraints. The FWHM was constrained to 2.7 eV for both components, and the binding energy of O 1s corresponding to the Si–O component was derived from the O 1s signal in SiO_2 prior to BCl_3/O_2 exposures. The deconvoluted O 1s spectrum [Fig. 2(b)] indicates the presence of both oxidized B and Si in the film at ~533.2 and ~532 eV, respectively, consistent with previously discussed results. This deconvolution also confirms that some O migrated from the SiO_2 substrate to contribute to the growing boron oxide film.[5]

B. BN cap deposition on B_2O_3/Si

The evolution of BN growth using BCl_3/NH_3 exposures at 600 K on B_2O_3/Si is displayed in Figs. 3(a)–3(d). The XPS data in Fig. 3(a) demonstrate that the first BCl_3/NH_3

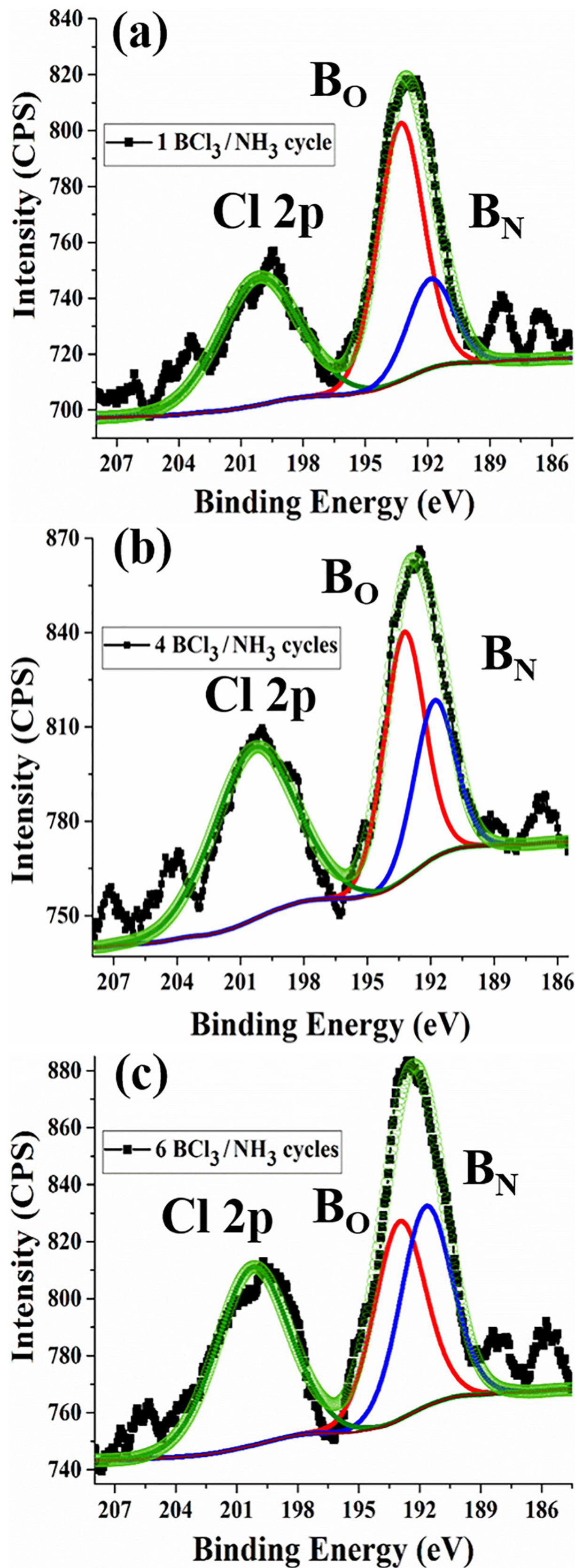

FIG. 4. Evolution of the B_O component (solid red line), the B_N component of B 1s (solid blue line), and Cl 2p (solid green line) XPS intensities (a) after 1 BCl_3/NH_3 cycle, (b) after 4 BCl_3/NH_3 cycles, and (c) after 6 BCl_3/NH_3 cycles at 600 K. The sum of the deconvoluted spectra (light green open circles) is in close agreement with experimental data (black square trace) in (a)–(c).

cycle results in a sharp decrease in the total B 1s signal at ~193.8 eV and a broadening of the B 1s feature toward a lower binding energy of ~192 eV. Subsequent BCl_3/NH_3 reaction cycles result in an increase in the broadened B 1s intensity and a further shift to 191.7 eV. The data in Fig. 3(a) also show an increase in the Cl 2p intensities with increasing number of BCl_3/NH_3 cycles. The data in Figs. 3(b) and 3(c) show a corresponding decrease in the O 1s intensity and an increase in the Si 2p intensity after the initial BCl_3/NH_3 exposures at 600 K. However, only a slight decrease is observed in the O 1s signal during the subsequent BCl_3/NH_3 cycles. Note that the decrease in O 1s intensities after 1 and 6 BCl_3/NH_3 reaction cycles [red circle and blue triangle traces in Fig. 3(b)], while experimentally distinct, is obscured by the relative intensity of the initial O 1s feature. Therefore, O 1s evolution is shown in more detail in Fig. S1 of the supplementary material.[27] The data in Fig. 3(d) demonstrate a monotonic growth of the N 1s feature at ~398.6 eV with increasing number of BCl_3/NH_3 reaction cycles. From the XPS survey scans, no nitrogen species were observed prior to the BN deposition. The shift in B 1s binding energy to lower values and the appearance of an N 1s signal at 398.6eV confirm the formation of BN on B_2O_3/Si.[15–17] The decrease in the B 1s and O 1s intensities during the first BCl_3/NH_3 cycle, and a corresponding increase in the Si 2p peak intensity, as seen in Figs. 3(a)–3(c), is consistent with the significant consumption of B_2O_3 during the initial BN deposition under these conditions. It should be noted that the consumption of B_2O_3 is marked by a decrease in XPS intensity at higher binding energies of 193.8 eV for B 1s and 532.8 eV for O 1s corresponding to B–OH bonds.[28] This suggests that the consumption of oxidized boron is mainly in the form of boric acid (H_3BO_3), but some B_2O_3 consumption cannot be ruled out. Although the B_2O_3 films were not exposed to air in between B_2O_3 and BN cap deposition, the presence of boric acid could be due to H_2O being used as a precursor during B_2O_3 film growth. The residual B 1s and O 1s peak maxima shift to lower binding energies of ~192.8 and ~532.3 eV, respectively.

The broad B 1s feature observed after BN cap deposition in Fig. 3(a) was deconvoluted into two peaks corresponding to B–O (denoted by B_O) and B–N (denoted by B_N) bonding environments by constraining the FWHM to 2.8 eV as shown in Fig. 4. Figures 4(a)–4(c) depict the deconvoluted spectra of B 1s and Cl 2p regions after 1, 4, and 6 BCl_3/NH_3 cycles at 600 K. These data demonstrate that the B 1s component corresponding to B_N at ~191.7 eV (Refs. 15–17) increases with increasing number of BCl_3/NH_3 cycles, indicating the growth of BN on B_2O_3.

The decrease in B_2O_3 average film thickness after the initial BCl_3/NH_3 exposures was calculated by first deconvoluting the B 1s spectrum into components corresponding to the oxide and nitride films (B_O, B_N) as shown in Figs. 4(a)–4(c) and then using the following equations for estimating the B_2O_3 [Eq. (1)] and BN [Eq. (2)] layer thicknesses:[20,29]

$$t_{B_2O_3} = \lambda_{Si \to B_2O_3} \times \ln\left(1 + \frac{I_{B_O}/ASF_B}{I_{Si}/ASF_{Si}}\right), \quad (1)$$

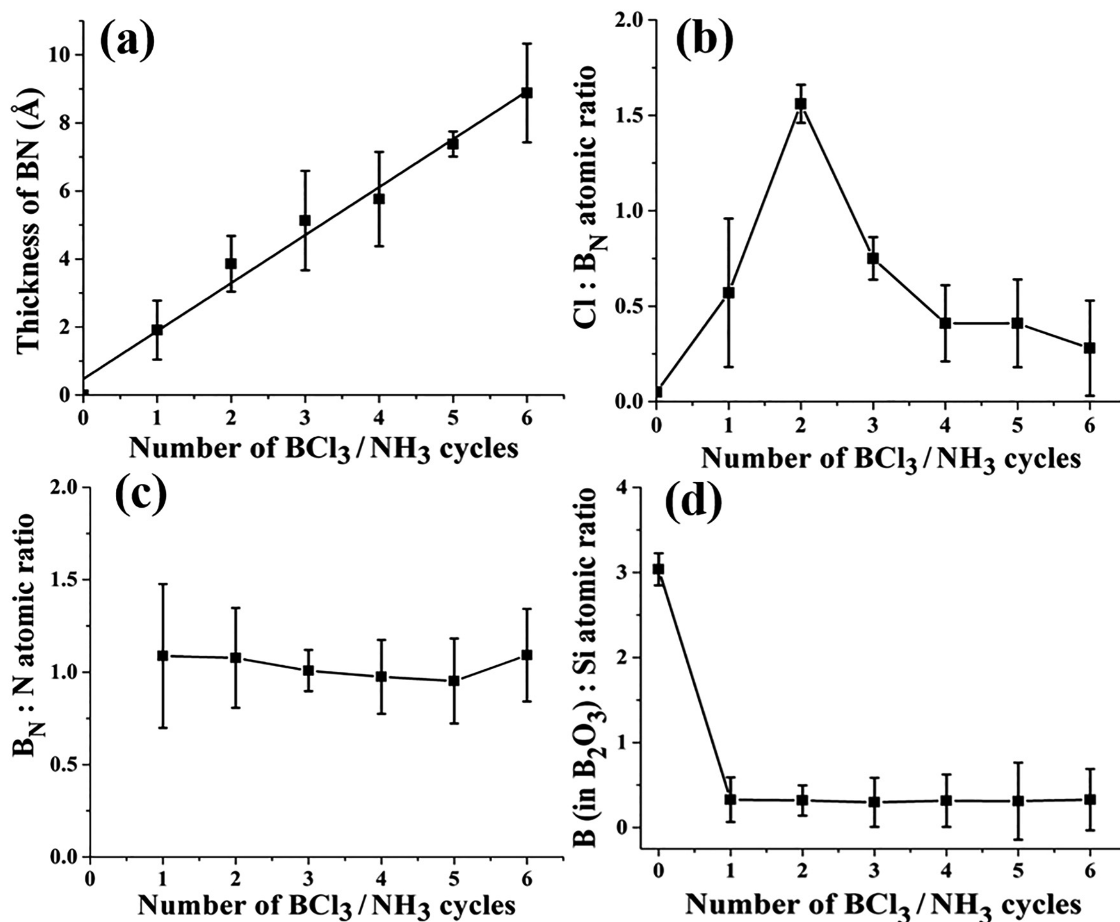

FIG. 5. BN deposition on B_2O_3/Si (a) XPS-derived BN film thickness, (b) the corresponding Cl to B_N atomic ratio, (c) B_N to N atomic ratio, and (d) the B_O (B in B_2O_3) to Si atomic ratio as a function of BCl_3/NH_3 cycles at 600 K.

$$t_{BN} = \lambda_{BO \to BN} \times \ln\left(1 + \frac{I_{B_N}/ASF_B}{I_{Si}/ASF_{Si}} \times \exp\left(-t_{B_2O_3}/\lambda_{Si \to B_2O_3}\right)\right). \quad (2)$$

Here, $t_{B_2O_3}$ and t_{BN} denote the thicknesses of B_2O_3 and BN films, respectively. The IMFP lengths used for Si through B_2O_3 ($\lambda_{Si \to B_2O_3}$) and B_O through BN ($\lambda_{BO \to BN}$) are 34.93 and 34.4 Å, respectively. The intensities used for these thickness calculations are denoted by I_{BO} and I_{BN} corresponding to the B_O and B_N components of the B 1s spectrum as shown in Figs. 4(a)–4(c). I_{Si} denotes the intensity of the Si 2p region as shown in Fig. 3(c). The atomic sensitivity factors of boron and silicon are denoted by ASF_B and ASF_{Si}, respectively.[20,29] The thickness of the BN layer calculated by this method [Eq. (2)] is of course dependent on the calculated thickness of the B_2O_3 layer [Eq. (1)].

The thickness of BN was also calculated using the attenuation of O 1s intensity obtained from B_2O_3 relative to the intensity of the N 1s spectrum, according to standard methods[20] [see Figs. 3(b) and 3(d) and Fig. S1 of the supplementary material].[27] This assumes that the consumption of B_2O_3 occurs only during the formation of the first complete BN layer. BN thickness calculations by this method agreed well with those computed using Eq. (2).[20,29] The boron oxide thickness decreased from ∼25.6 ± 1.4 to ∼13 ± 1 Å after 1 BCl_3/NH_3 cycle at 600 K with no further loss during the subsequent cycles.

The evolution of XPS-derived average BN film thickness with the number of BCl_3/NH_3 cycles at 600 K is displayed in Fig. 5(a). Corresponding Cl/B_N, B_N/N, and B_O/Si atomic ratios as a function of the number of BCl_3/NH_3 reaction are displayed in Figs. 5(b)–5(d), respectively. Figure 5(a) shows a linear, ALD-type growth of BN with growth rates directly proportional to the number of BCl_3/NH_3 cycles at 600 K. The average growth rate of BN on B_2O_3 is ∼1.4 ± 0.2 Å/cycle, which is consistent with results obtained for BN ALD using BCl_3/NH_3 precursors on Co,[15,16] RuO_2,[17] and ZrO_2 (Ref. 12) substrates. Data in Fig. 5(b) indicate an initial Cl/B_N atomic ratio of 0.05, corresponding to a monolayer of Cl residue seen during B_2O_3 growth at the B_2O_3–Si interface.[5] The Cl to B_N atomic ratio is observed to increase up to 2 BCl_3/NH_3 cycles, followed by a decrease during subsequent BCl_3/NH_3 exposures at 600 K. The continuous removal of Cl with increasing number of BCl_3/NH_3 cycles suggests that the NH_3 exposures at 350 mTorr for 2 min are not saturation-limiting on the B_2O_3/Si surface under these deposition conditions. The residual Cl impurity was reduced significantly after a 10 min anneal to 800 K in UHV, with no significant change in the B 1s or N 1s XPS spectra.

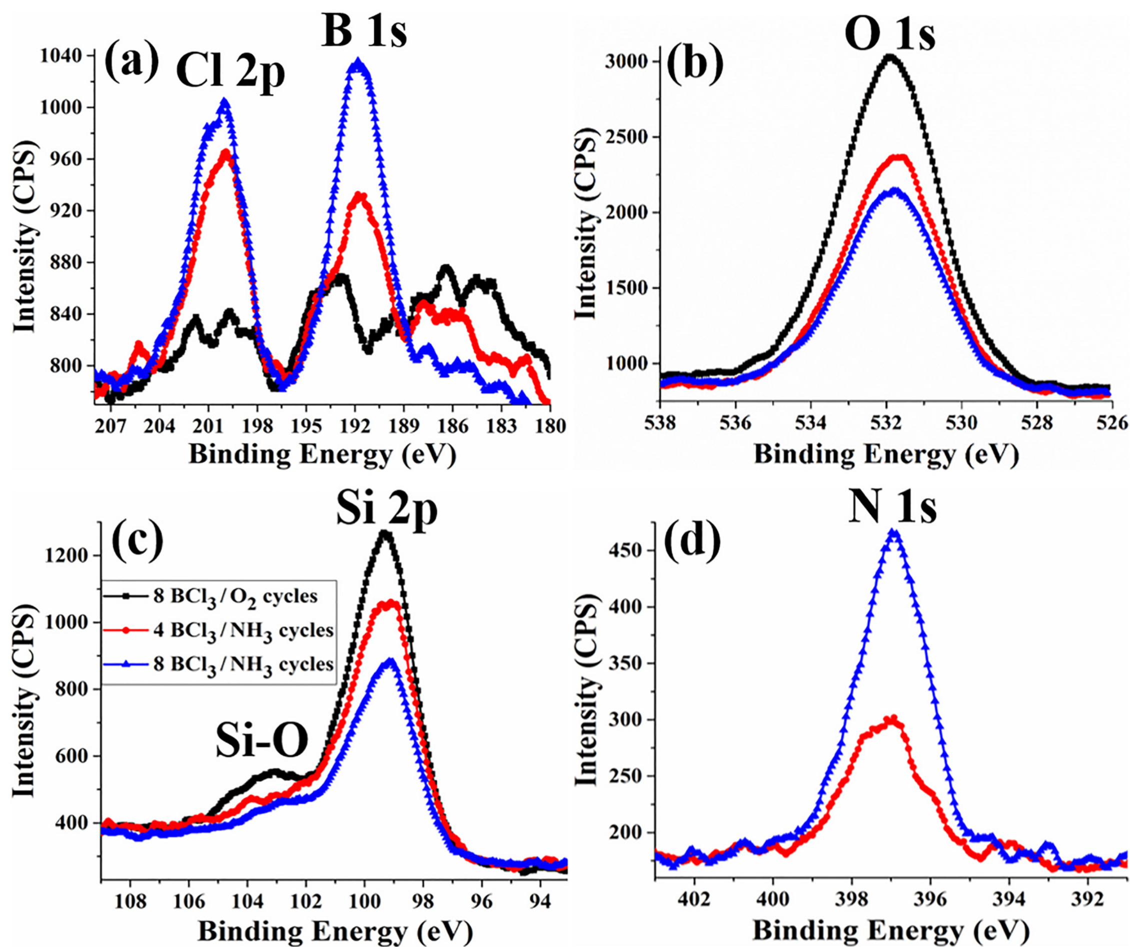

FIG. 6. Evolution of (a) B 1s and Cl 2p, (b) O 1s, (c) Si 2p, and (d) N 1s XPS spectra during BN ALD at 600 K on a B-Si-oxide film. After 8 BCl_3/O_2 cycles at 650 K and 0 BCl_3/NH_3 cycles (black square trace), after 4 BCl_3/NH_3 cycles (red circle trace), and after 8 BCl_3/NH_3 cycles (blue triangle trace) at 600 K.

The data in Fig. 5(c) indicate stoichiometric BN film formation with the B_N to N atomic ratio ∼1:1. Data in Fig. 5(d) show the ratio of B_O to Si decreases significantly upon the first cycle of BCl_3/NH_3 corresponding to the decrease in B_2O_3 film thickness from ∼25.6 ± 1.4 to ∼13 ± 1 Å. After the first BCl_3/NH_3 cycle, the ratio does not decrease further, indicating that the consumption of B_2O_3 layer was limited to the initial BCl_3/NH_3 exposures.

C. BN cap deposition on B-Si-oxide

The evolution of BN growth using BCl_3/NH_3 exposures at 600 K on B-Si-oxide films deposited on SiO_2 is displayed in Figs. 6(a)–6(d). The data in Fig. 6(a) demonstrate an increase in the B 1s intensity and a shift in the binding energy from 193.6 to 191.4 eV after BCl_3/NH_3 cycling at 600 K.[15–17] Peak broadening toward lower binding energies was observed corresponding to an increase in the FWHM from 2.5 to 3 eV with increasing number of BCl_3/NH_3 cycles. The O 1s and Si 2p spectra in Figs. 6(b) and 6(c) indicate negligible consumption of B-Si-oxide during the BN deposition. The decrease in O 1s intensity [Fig. 6(b)] is consistent with the attenuation of XPS signal caused by the BN overlayer. Figure 6(d) shows a monotonic increase in the N 1s intensity at ∼397.2 eV with increasing number of BCl_3/NH_3 cycles. From the XPS survey scans, no nitrogen species were observed prior to BN deposition.

These results indicate that ∼12.8 ± 0.2 Å of the BN film was deposited after 8 BCl_3/NH_3 cycles on ∼7.8 ± 0.2 Å of B-Si-oxide without erosion of the underlying layer. The increase in the FWHM of B 1s after BN ALD on B–O–Si also indicates the presence of two different bonding environments corresponding to both B–O (Refs. 5 and 22) and B–N (Refs. 15–17) species.

D. Thermal and ambient stability of $BN/B_2O_3/Si$

The thermal stability of $BN/B_2O_3/Si$ heterostructures was examined by annealing a $BN/B_2O_3/Si$ sample prepared under identical conditions to those discussed in Sec. II B. This sample had a BN film thickness of ∼13 ± 0.2 Å, deposited after 8 BCl_3/NH_3 cycles at 600 K on a B_2O_3 layer deposited using 11 BCl_3/H_2O cycles at 300 K. Postdeposition annealing was done to ∼800 K to remove the residual Cl impurities from the BN film. The XPS spectra of B 1s and Cl 2p regions before and after the anneal are shown in Fig. S2 of the supplementary material.[27] In order to test the thermal stability of these heterostructures, the film was then annealed to ∼1130 K in UHV for

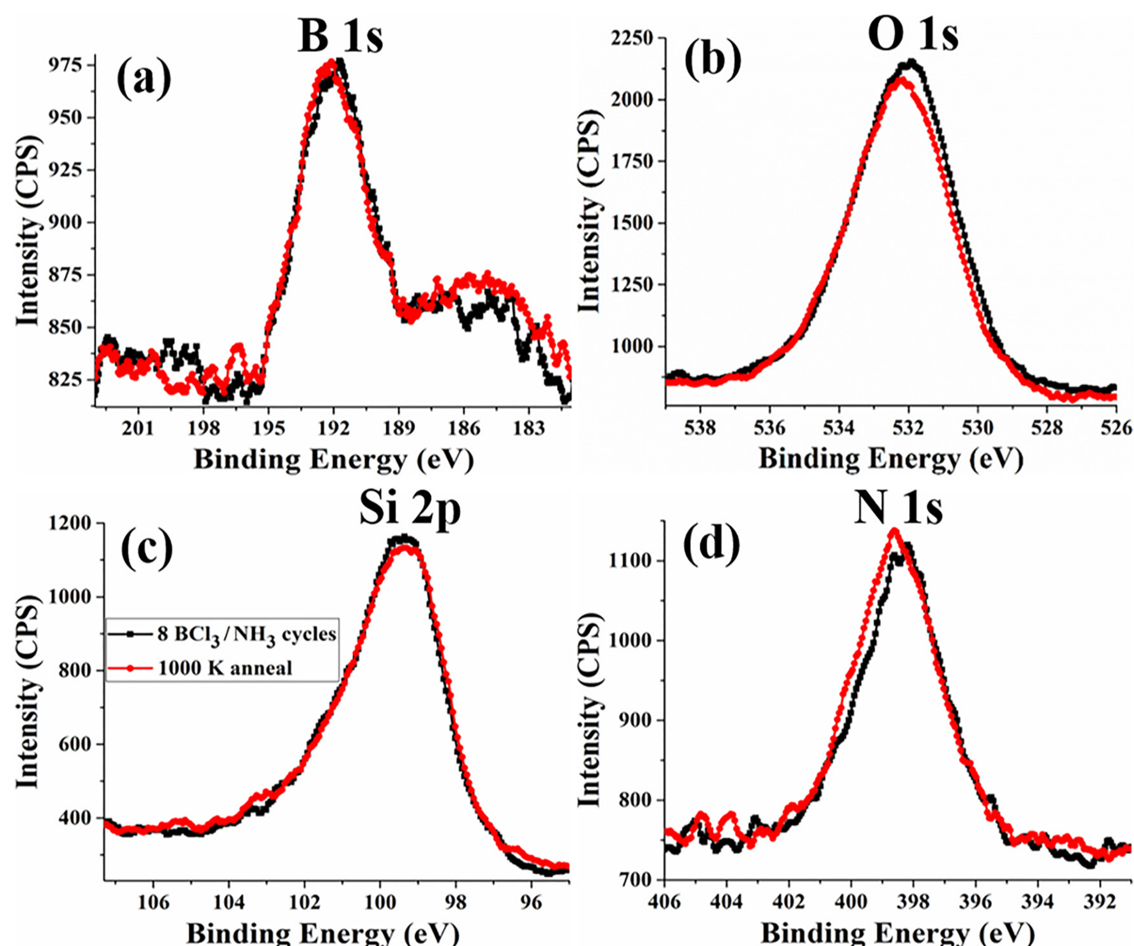

FIG. 7. Evolution of (a) B 1s, (b) O 1s, (c) Si 2p, and (d) N 1s XPS spectra after 8 BN ALD cycles on B_2O_3/Si (black square trace) and after 30 min UHV anneal to >1000 K (red circle trace).

30 min (Fig. 7). The data in Figs. 7(a)–7(d) show no significant change in the core level XPS spectra of B 1s, O 1s, Si 2p, and N 1s regions. The B 1s peak maxima did not shift to lower binding energy (~187–188 eV) to suggest Si–B bond formation in Fig. 7(a).[30] The reason for no observable doping might be due to our low anneal temperatures. The minimum temperature used for thermal activation and dopant drive-in is ~1173 K.[1–3] Another reason for the lack of shift in the B 1s binding energy might also be due to the absence of a controlled temperature gradient usually applied for a short duration during RTA treatment required for dopant activation.[1–3] The data in Fig. 7, however, indicate that the BN/B_2O_3/Si heterostructure is thermally stable to ~1130 K in UHV.

The ambient stability of BN-capped B_2O_3 films was examined by exposing the annealed sample to atmosphere at room temperature for ~5 min. Uncapped B_2O_3 films react readily with the atmospheric moisture, resulting in volatile boric acid formation upon exposure.[1–4,6] The evolution of B 1s, O 1s, and N 1s spectra before and after ambient exposure is shown in Figs. 8(a)–8(c). The binding energy of H_3BO_3 is ~194 eV, which is about 1 eV higher than that of B_2O_3 (~193 eV).[3,28,31,32] The B 1s spectrum in Fig. 8(a) shows no shift to higher binding energy or broadening of the peak that would suggest boric acid formation. Figure 8(b) indicates a significant increase in O 1s intensity and a slight shift to lower binding energy at ~532 eV. Figure 8(c) shows the N 1s region before and after ambient exposure. A significant attenuation in the N 1s intensity and the appearance of small shoulder at a binding energy of ~401.3 eV corresponding to N–O species is observed upon ambient exposure.[33] In order to elucidate the effect of ambient exposure on N sites, the N 1s spectra before and after ambient exposure were deconvoluted into two peaks. Before exposure, the two components correspond to N–B (Refs. 15–17) and N–H (Ref. 33) bonding environments centered at ~398.4 and ~399.3 eV using the FWHM constraint [see Fig. S3(a) of the supplementary material].[27] The existence of NH_x species at BN surfaces prepared by BCl_3/NH_3 ALD has been identified by FTIR.[10,12] Oxidation of these surface NH_x species results in NO formation, as indicated by a broad shoulder at ~401.3 eV [Fig. S3(b)].[27,32] However, the unchanged nature of peak at ~398.4 eV corresponding to B–N after ambient exposure [Fig. S3(b)],[27] as well as the unchanged B 1s feature [Fig. 8(a)], demonstrates that exposure to ambient leaves the BN framework intact.

The consistency of the B 1s spectrum upon ambient exposure [Fig. 8(a)] and the lack of broadening in the O 1s spectrum would indicate hydroxylation or boric acid formation.

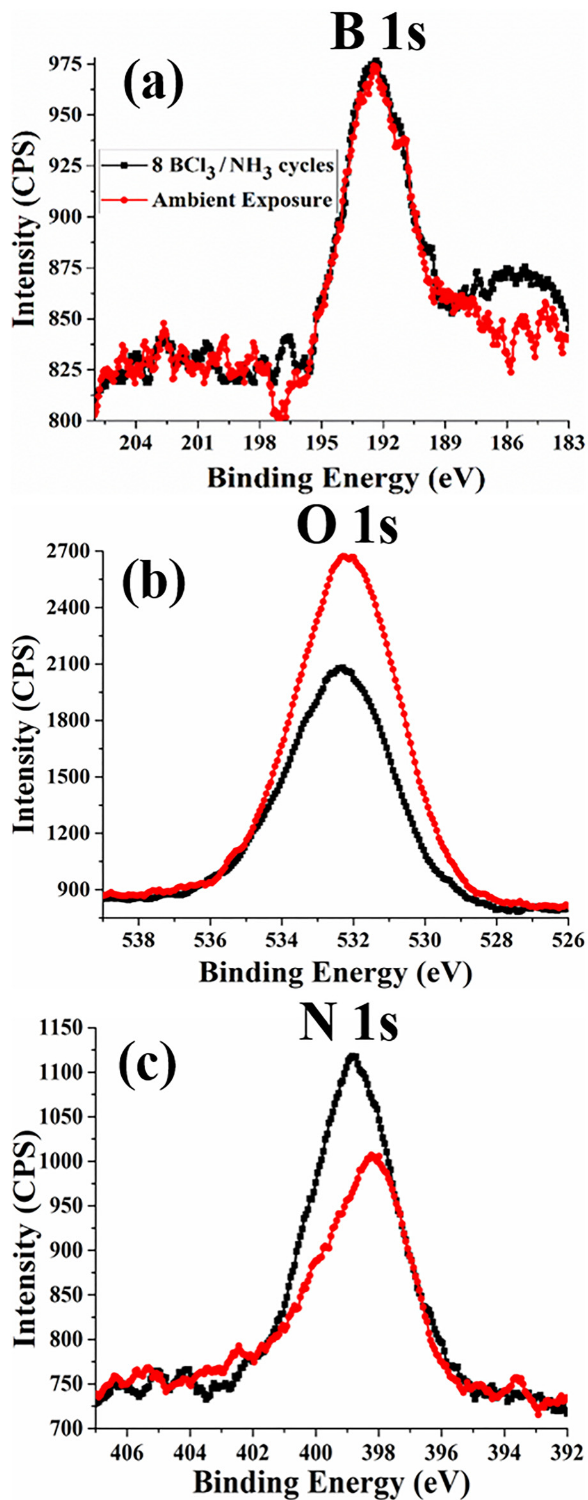

FIG. 8. Evolution of (a) B 1s, (b) O 1s, and (c) N 1s XPS spectra after 8 BCl_3/NH_3 cycles on B_2O_3/Si (black square trace) and after ambient exposure at room temperature (red circle trace).

Figure 8(b) also demonstrates that reaction with ambient is confined to NH_x sites at the BN surface. The BN film successfully passivates the boron oxide substrate from moisture contamination under these atmospheric conditions.

The results in Figs. 7(a)–7(d) and 8(a)–8(c) demonstrate that ~13 ± 0.2 Å of BN is sufficient to passivate B_2O_3 films deposited on Si from moisture contamination, and the films were also found to be stable at temperatures close to those used for doping applications. These results, therefore, indicate that BN acts as an excellent capping barrier for B_2O_3.

E. Thermal and ambient stability of BN/B-Si-oxide

The thermal stability of BN/B-Si-oxide heterostructures was examined by annealing the films in UHV to 1000 K for 1 h. The XPS spectra of B 1s and Cl 2p regions after BN cap deposition on B-Si-oxide followed by a UHV anneal to ~1000 K are shown in Fig. 9(a). The corresponding O 1s, Si 2p, and N 1s spectra are displayed in Figs. 9(b)–9(d), respectively. Figure 9(a) shows no significant change in the intensity of B 1s region after the anneal. However, the residual Cl was removed from the BN film, which also resulted in a slight shift in the binding energy of the B 1s feature from 190.9 to 191.3 eV. This observation is consistent with the breaking of B–Cl bonds,[34] and the binding energy of B 1s after the anneal corresponds to B–N species.[15–17] Figure 9(d) also shows a slight intensity decrease in the N 1s region corresponding to some loss of BN during the anneal process. Figures 9(b) and 9(c) demonstrate a slight increase in the intensity of O 1s and Si 2p regions corresponding to Cl removal from the BN film.

The ambient stability of BN-capped B-Si-oxide films was examined by exposing the samples to atmosphere at room temperature for ~5 min. The corresponding XPS data of the B 1s, O 1s, and N 1s regions are displayed in Figs. 10(a)–10(c), respectively. The B 1s feature in Fig. 10(a) showed no significant shift to higher binding energy to suggest oxidation or hydroxylation upon ambient exposure. Figure 10(b) indicates a significant increase in O 1s intensity at ~532 eV. Figure 10(c) shows attenuation in the N 1s intensity upon ambient exposure and a narrowing of the N 1s feature toward lower binding energies. These changes are similar to those observed upon the exposure of BN/B_2O_3/Si films to ambient [Fig. 8(c)].

The changes in O 1s and N 1s intensities evident in Figs. 10(b) and 10(c) can be understood by the deconvolution of N 1s spectrum before and after ambient exposure [Figs. S4(a) and S4(b) of the supplementary material],[27] which are similar to those observed upon ambient exposure of BN/B_2O_3 [Fig. 8(c) and Figs. S4(a) and S4(b)].[27] The N1s spectrum prior to ambient exposure can again be deconvoluted into components centered at ~397.0 eV corresponding to N–B (Refs. 15–17) and at ~398.0 eV corresponding to N–H (Ref. 33) bonding environments, as shown in Fig. S4(a).[27] The N 1s spectrum after ambient exposure [Fig. S4(b)][27] is again well fit by a decrease in the intensity of the NH_x feature and the addition of a small shoulder at 400.1 eV corresponding to N–O bond formation.[34] The B–N component at a lower binding energy of 397.0 eV again remains unchanged upon exposure [Figs. S4(a) and S4(b)],[27] indicating that the BN framework remains intact with some oxidation at the surface NH_x species. This interpretation is also consistent with the lack of change in the B 1s peak binding energy or width upon ambient exposure [Fig. 10(a)].

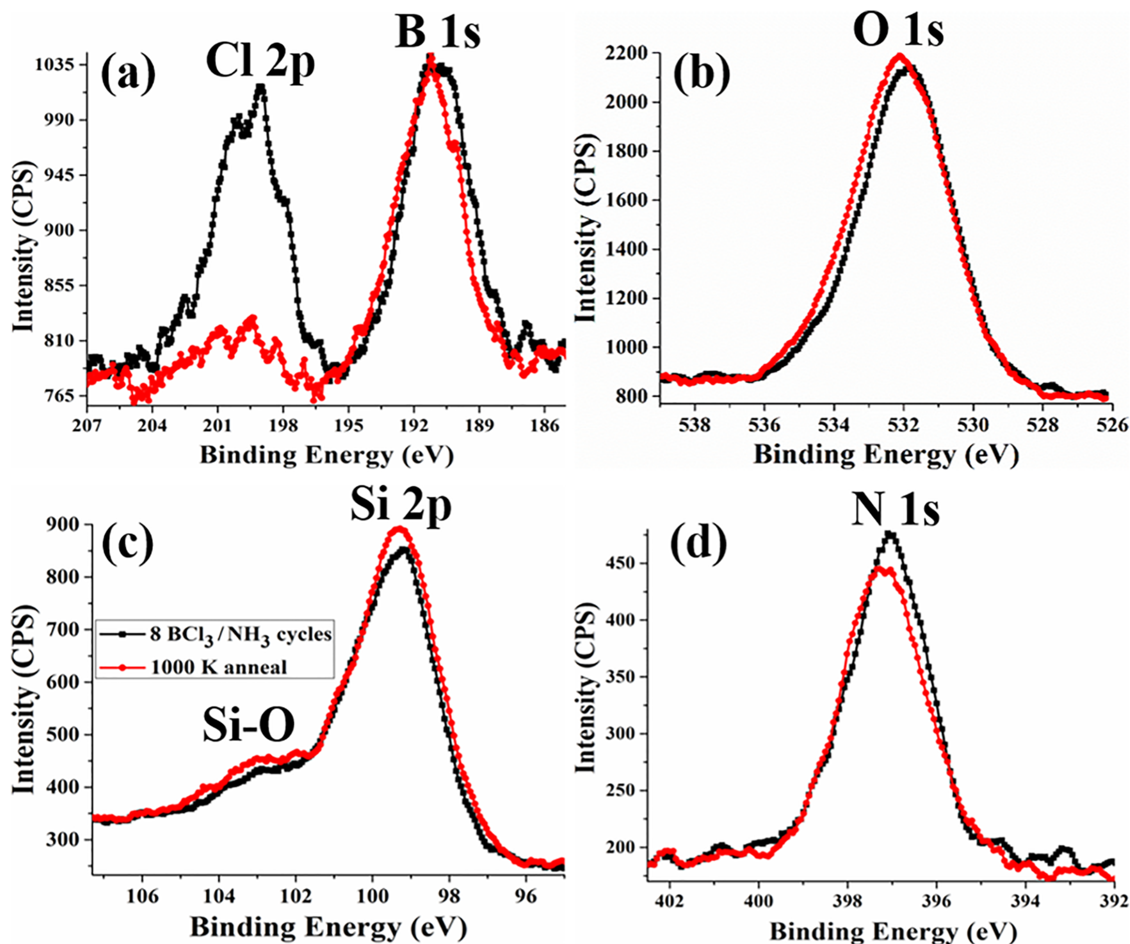

Fig. 9. Evolution of (a) B 1s and Cl 2p, (b) O 1s, (c) Si 2p, and (d) N 1s XPS spectra after 8 BCl_3/NH_3 cycles on B-Si-oxide (black square trace) and after 1 h UHV anneal to 1000 K (red circle trace).

The data in Figs. 10(a)–10(c) and Figs. S3(a) and S3(b)[27] indicate that ambient exposure results in some oxidation at N sites—attributable to the reaction of surface NH_x groups—but that no hydroxylation or boric acid formation is observed at B sites. These data, therefore, demonstrate that ∼12.8 ± 0.2 Å of BN is sufficient to passivate ∼7.8 ± 0.2 Å B-Si-oxide films from moisture contamination during a brief room temperature exposure to ambient.

IV. DISCUSSION

The loss of B_2O_3 upon the reaction of B_2O_3/Si with BCl_3/NH_3 occurs only during the first BCl_3/NH_3 cycle [Figs. 3(a) and 5(d)], but no such loss is observed on B-Si-oxide films. This result is consistent with the findings of Basu *et al.*, who observed partial conversion of B_2O_3 films to BN by reaction with NH_3 over a range of temperatures up to ∼1573 K.[35] That study determined that the maximum amount of B_2O_3 converted to BN was between 64% and 66% at temperatures >1223 K,[35] which in good agreement with our data indicating that ∼54% of B_2O_3 was converted to BN (Figs. 3–5). Another study by Ferguson *et al.* established the removal of surface hydroxyl groups on ZrO_2 after the first BCl_3 exposure during BN ALD.[12] These studies and our own results strongly suggest that further loss of B_2O_3 is limited by the formation of a continuous BN overlayer.

Since the dopant concentration is dependent on the thickness of the B_2O_3 layer, a much thicker initial B_2O_3 film than those used in this study is typically required to achieve the desired dopant concentration.[1,2] Our results indicate that the limited loss of B_2O_3, about 13 ± 1 Å film thickness, may well be acceptable in the development of BN as a practical passivation barrier.

The data presented in Fig. 6 also indicate that BCl_3/NH_3 reaction cycles at 600 K did not cause a reaction of the B-Si-oxide. Kim *et al.* concluded that such mixed oxide films are suitable for RTA procedures.[3] The data presented here show that such B-Si-oxide films deposited on SiO_2 using BCl_3/O_2 cycles at 650 K are both thermally stable to ∼1000 K in UHV and chemically stable toward NH_3 exposures at ∼600 K.

Previous studies have explored the use of various oxides, including Al_2O_3,[1,6] Sb_2O_5,[2,4] or SiO_2,[3,7] as B_2O_3 passivation barriers. These barriers have shown inability to passivate the surface against moisture contamination. Al_2O_3 capping barrier showed signs of cracking at temperatures >673 K.[6] Sb_2O_5 is also volatile at elevated temperatures and hence is unsuitable for RTA experiments.[4] These caps also failed to passivate the underlying B_2O_3 films from moisture contamination resulting

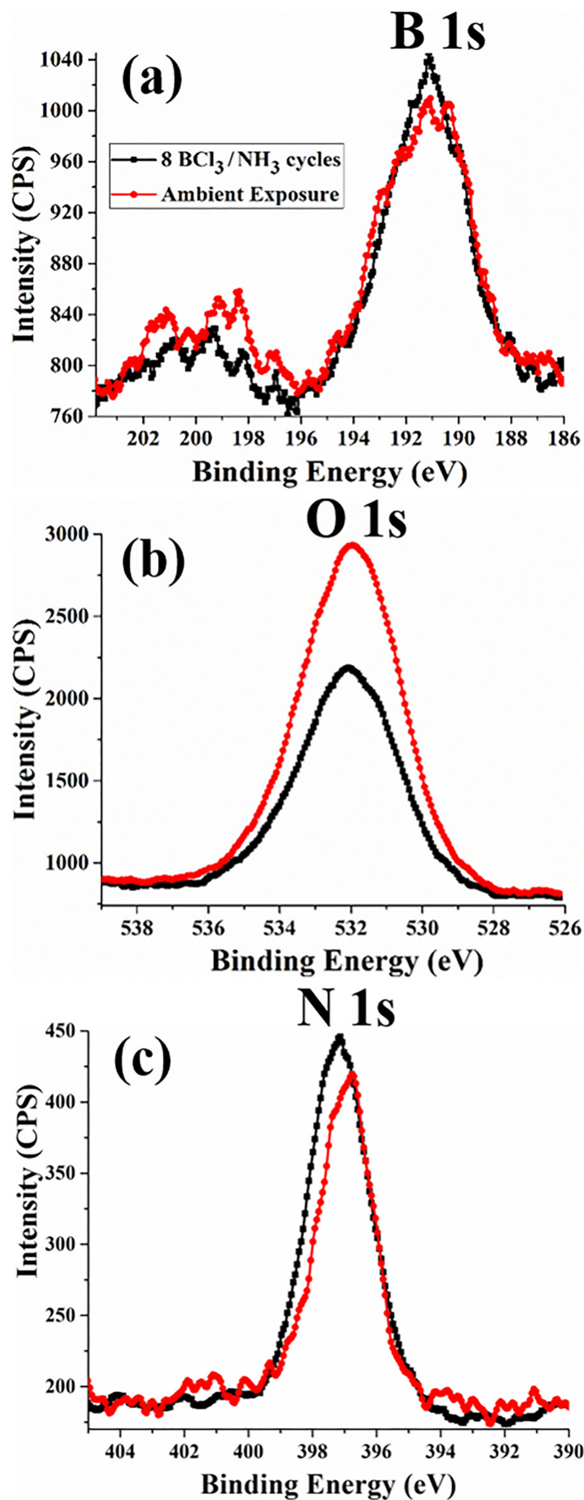

FIG. 10. Evolution of (a) B 1s and Cl 2p, (b) O 1s, and (c) N 1s XPS spectra after 8 BN ALD cycles on B-Si-oxide (black square trace) and after ambient exposure at room temperature (red circle trace).

in boric acid formation.[2,6] Both Al_2O_3 and SiO_2 form mixed oxides with B_2O_3 during cap deposition.[4] This results in a loss of control over dopant source layer thickness, which, in turn, affects B dopant concentration. B dopants are also known to diffuse into the SiO_2 sidewall spacers at RTA temperatures, resulting in a loss of B dosage.[7]

The data presented here demonstrate the feasibility of BN film deposition on either B_2O_3 or B-Si-oxide substrates and also indicate the potential suitability of even very thin (∼13 ± 0.2 Å thick) BN films as passivation barriers against brief exposures to ambient at room temperature. BN as a capping barrier may prevent upward boron diffusion into the cap at elevated temperatures, thus preventing the loss of dopant concentration.

V. SUMMARY AND CONCLUSIONS

Stoichiometric BN films have been deposited by sequential BCl_3/NH_3 reactions at 600 K on B_2O_3 films deposited on Si and on B-Si-oxide films formed by BCl_3/O_2 reactions with SiO_2 at elevated temperatures. The data show that BN growth on a 25.6 ± 1.4 Å thick B_2O_3 film results in the consumption of about 13 ± 1 Å of B_2O_3 during the first BCl_3/NH_3 cycle but with no further B_2O_3 consumption during subsequent cycles. BN growth on B-Si-oxide films resulted in no significant reaction with or consumption of the substrate.

BN overlayers of ∼13 ± 0.2 Å thick on both types of oxide substrates remained stable upon annealing to 1000 K in UHV. Brief (∼5 min) exposures to ambient at room temperature yielded some oxidation of the BN film at surface NH_x sites, but without observable reaction at the B sites corresponding to the boron nitride overlayer or the boron oxide substrate layer. The data presented here, therefore, demonstrate that ultrathin BN films deposited by BCl_3/NH_3 ALD are promising candidates for passivation of boron oxide used in shallow doping applications.

ACKNOWLEDGMENTS

This work was partially supported by a grant from Lam Research, Inc., which is gratefully acknowledged. A.P. and J.J. also acknowledge support from the UNT College of Science in the form of summer research fellowships.

[1]S. Consiglio, R. D. Clark, D. O'Meara, C. S. Wajda, K. Tapily, and G. J. Leusink, J. Vac. Sci. Technol. A **34**, 01A102 (2016).
[2]B. Kalkofen, A. A. Amusan, M. Bukhari, B. Garke, M. Lisker, H. Gargouri, and E. P. Burte, J. Vac. Sci. Technol. A **33**, 031512 (2015).
[3]W. Kim *et al.*, J. Mater. Chem. C **2**, 5805 (2014).
[4]B. Kalkofen, V. M. Mothukuru, M. Lisker, and E. P. Burte, ECS Trans. **45**, 55 (2012).
[5]A. Pilli, J. Jones, V. Lee, N. Chugh, J. Kelber, F. Pasquale, and A. LaVoie, J. Vac. Sci. Technol. A **36**, 061503 (2018).
[6]M. Putkonen and L. Niinisto, Thin Solid Films **514**, 145 (2006).
[7]Z. Essa *et al.*, Solid State Electron. **126**, 163 (2016).
[8]N. Biyikli and A. Haider, Semicond. Sci. Technol. **32**, 093002 (2017).
[9]B. Marlid, M. Ottosson, U. Pettersson, K. Larsson, and J.-O. Carlsson, Thin Solid Films **402**, 167 (2002).
[10]J. Olander, L. M. Ottosson, P. Heszler, J. O. Carlsson, and K. M. E. Larsson, Chem. Vap. Deposition **11**, 330 (2005).
[11]M. Weber, B. Koonkaew, S. Balme, I. Utke, F. Picaud, I. Iatsunskyi, E. Coy, P. Miele, and M. Bechelany, ACS Appl. Mater. Interfaces **9**, 16669 (2017).
[12]J. D. Ferguson, A. W. Weimer, and S. M. George, Thin Solid Films **413**, 16 (2002).
[13]M. Snure, Q. Paduano, M. Hamilton, J. Shoaf, and J. M. Mann, Thin Solid Films **571**, 51 (2014).
[14]H. Park, T. K. Kim, S. W. Cho, H. S. Jang, S. I. Lee, and S. Choi, Sci. Rep. **7**, 1 (2017).

[15]J. Beatty, Y. Cao, I. Tanabe, M. S. Driver, P. A. Dowben, and J. A. Kelber, Mater. Res. Express **1**, 46410 (2014).
[16]M. S. Driver, J. D. Beatty, O. Olanipekun, K. Reid, A. Rath, P. M. Voyles, and J. A. Kelber, Langmuir **32**, 2601 (2016).
[17]J. Jones, B. Beauclair, O. Olanipekun, S. Lightbourne, M. Zhang, B. Pollok, A. Pilli, and J. Kelber, J. Vac. Sci. Technol. A **35**, 01B139 (2017).
[18]J.-W. He, X. Xu, J. S. Corneille, and D. W. Goodman, Surf. Sci. **279**, 119 (1992).
[19]C. D. Wagner, D. E. Passoja, H. F. Hillery, T. G. Kinisky, H. A. Six, W. T. Jansen, and J. A. Taylor, J. Vac. Sci. Technol. **21**, 933 (1982).
[20]M. P. Seah, D. Briggs, and M. P. Seah, "Quantification of AES and XPS," in *Practical Surface Analysis: Auger and X-ray Photoelectron Spectroscopy*, 2nd ed. (Wiley, West Sussex, 1997), Vol. 1, pp. 200–255.
[21]S. Tanuma, C. J. Powell, and D. R. Penn, Surf. Interface Anal. **35**, 268 (2003).
[22]Y. Wang and M. Trenary, Chem. Mater. **5**, 199 (1993).
[23]E. J. Nemanick, P. T. Hurley, L. J. Webb, D. W. Knapp, D. J. Michalak, B. S. Brunschwig, and N. S. Lewis, J. Phys. Chem. B **110**, 14770 (2006).
[24]P. Melinon, P. Keghelian, B. Prevel, A. Perez, G. Guiraud, J. LeBrusq, J. Lerme, M. Pellarin, and M. Broyer, J. Chem. Phys. **107**, 10278 (1997).
[25]Y. Saito and A. Yoshida, J. Electrochem. Soc. **139**, L115 (1992).
[26]Y. I. Matyunin, S. V. Yudintsev, and Y. P. Dikov, *WM'00 Conference*, Tucson, AZ, 27 February–2 March 2000 (available online at http://archive.wmsym.org/2000/pdf/41/41-28.pdf)
[27]See supplementary material at https://doi.org/10.1116/1.5092806 for the XPS of O 1s after 1 and 6 BCl_3/NH_3 cycles, XPS of B 1s and Cl 2p regions after 8 BCl_3/NH_3 cycles followed by 800 K UHV anneal, XPS of deconvoluted N 1s from $BN/B_2O_3/Si$ heterostructure before and after exposure to ambient, and XPS of deconvoluted N 1s from BN/B-Si-oxide heterostructure before and after ambient exposure.
[28]K. Yao, X. Lu, J. Feng, J. Ouyang, and Y. Tian, Vacuum **117**, 68 (2015).
[29]M. J. Dreiling, Surf. Sci. **71**, 231 (1978).
[30]M. Fujii, H. Sugimoto, M. Hasegawa, and K. Imakita, J. Appl. Phys. **115** (2014).
[31]B. A. Cook, J. L. Harringa, J. Anderegg, A. M. Russell, J. Qu, P. J. Blau, C. Higdon, and A. A. Elmoursi, Surf. Coat. Technol. **205**, 2296 (2010).
[32]X. Gouin, P. Grange, L. Bois, P. L'Haridon, and Y. Laurent, J. Alloys Compd. **224**, 22 (1995).
[33]M. Grunze, C. R. Brundle, and D. Tomanek, Surf. Sci. **119**, 133 (1982).
[34]A. A. Kobelev, Y. V. Barsukov, N. A. Andrianov, and A. S. Smirnov, J. Phys. Conf. Ser. **586**, 4 (2015).
[35]A. K. Basu and J. Mukerji, Bull. Mater. Sci. **13**, 165 (1990).